Growth Mechanism of Metal Clusters on a Graphene/Ru(0001) Template

L. Z. Zhang, S. X. Du, J. T. Sun, L. Huang, L. Meng, W. Y. Xu, L. D. Pan, Y. Pan, Y. L. Wang, W. A. Hofer, and H.-J. Gao*

Using first-principles calculations combined with scanning tunneling microscopy experiments, we investigated the adsorption configurations, electronic structures and the corresponding growth mechanism of several transition metal (TM) atoms (Pt, Ru, Ir, Ti, Pd, Au, Ag, and Cu) on a graphene/Ru(0001) moiré template (G/Ru(0001)) at low coverage. We find that Pt, Ru, Ir, and Ti selectively adsorb on the fcc region of G/Ru(0001) and form ordered dispersed metal nanoclusters. This behavior is due to the unoccupied *d* orbital of the TM atoms and the strong sp^3 hybridization of carbon atoms in the fcc region of G/Ru(0001). Pd, Au, Ag, and Cu form nonselective structures because of the fully occupied *d* orbital. This mechanism can be extended to metals on a graphene/Rh(111) template. By using Pt as an example, we provide a layer by layer growth path for Pt nanoclusters in the fcc region of the G/Ru(0001). The simulations of growth mechanism agree well with the experimental observations. Moreover, they also provide guidance for the selection of suitable metal atoms to form ordered dispersed metal nanoclusters on similar templates.

1. Introduction

Metal nanoclusters have attracted considerable interest because of the potential applications in catalysis and information storage.[1–3] The intrinsic size, shape and pattern of clusters have strong influence on their activity, selectivity and the efficiency of the catalyst.[3] How to control these factors effectively or cooperatively is of great importance and remains a big challenge.[3,4] Recently, thin film templates or patterned substrates have been proposed as an effective base for selective growth of homogenous and size-controlled metal nanoclusters.[5–7] Another potential base, which will be investigated here, is epitaxial graphene. Due to the soft nature of epitaxial graphene and the lattice mismatch between graphene and metal substrates periodic moiré patterns can be formed.[8–12] Within one period of each moiré pattern, the electronic structure of carbon atoms at different locations varies due to the distinct interactions between hexagonal carbon rings of epitaxial graphene and the metal substrate.[13–15] One expects, therefore, that the adsorption behavior of adsorbates should be different at different regions of the moiré pattern.[6,7,15] For example, a graphene/metal template (G/metal) can be used to grow organic molecules,[16,17] dispersed metal nanoclusters with controllable size and shape, or metal clusters with large size and metal layers. Among the systems reported so far are Ir, Pt, W, Re, and Rh nanoclusters on G/Ir(111),[6,7,18,19] or Pt, Ru, and Pd nanoclusters on G/Ru(0001),[20–23] or Ni nanoclusters on G/Rh(111).[24] Other experimental groups found that Pd and Co (Au) will form large clusters (metal film) on a G/Ru(0001).[25,26]

The growth mechanisms of the metal clusters on these templates at the atomic scale can be analyzed using density functional theory (DFT). For example, it was found by Feibelman that the local sp^3 re-hybridization of carbon atoms in G/Ir(111) controls the adsorption of Ir clusters; the three dimensional Ir clusters become energetically stable when the number of metal atoms increases.[27,28] Wang *et al.* have reported that the competition between the transition metal (TM)-graphene (G) and TM-TM interactions controls the morphology of TM clusters grown on G/Ru(0001).[29] However, how intrinsic properties of TM atoms and the moiré template influence the selective adsorption and the growth mode of TM clusters is still open to debate. A general rule, predicting the morphology of metal nanoclusters on a G/metal surface, important to guide experimenters, is still missing.

Aiming at such a more general rule, we studied the adsorption behavior and growth modes of Pt, Ru, Ir, Ti, Pd, Au, Ag, and Cu on G/Ru(0001) at their initial growth stages by *ab-initio* calculations based on DFT. We found that both the sp^3 hybridization of carbon atoms at the fcc region of G/Ru(0001) and the occupation of the *d* orbital of the metal atoms control the growth mode of the metal atoms on G/Ru(0001). By using Pt as an example, we also studied the detailed growth process of the dispersed Pt nanoclusters at the fcc region of G/Ru(0001). Our simulated results fully agree with the experimental observations.

Dr. L. Z. Zhang, Prof. S. X. Du, Prof. J. T. Sun, Dr. L. Huang, Dr. L. Meng, W. Y. Xu, L. D. Pan, Dr. Y. Pan, Prof. Y. L. Wang, Prof. H.-J. Gao
Institute of Physics, Chinese Academy of Sciences
Beijing 100190, P. R. China
E-mail: sxdu@iphy.ac.cn

Prof. W. A. Hofer
Department of Physics, the University of Liverpool
Liverpool, L69 3BX, UK

DOI: 10.1002/admi.201300104

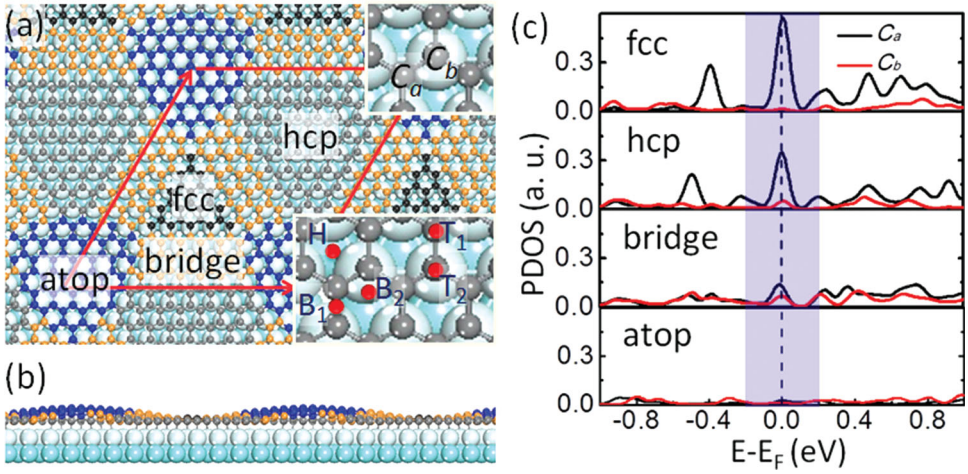

Figure 1. Configuration and projected density of states of graphene on Ru(0001): Top (a) and side (b) view of the configuration of G/Ru(0001). The top-right inset in (a) shows two types of carbon atoms, C_a on the hollow site and C_b on the top site of the first layer of Ru(0001). The bottom-right inset in (a) indicates typical adsorption sites for one metal atom on G/Ru(0001) using the red dots. H, T and B denote the hole, top and bridge site. The carbon atoms in hcp, fcc, atop and bridge regions of G/Ru(0001) are denoted by small balls with green, black, blue and yellow, respectively. (c) The projected density of states on p_z orbital of C_a and C_b in different regions of G/Ru(0001).

2. Results and Discussion

For the G/Ru(0001) system, the calculation of the electronic structure using GGA at fcc and hcp regions have been reported.[29,30] However, the dispersion forces are neglected in these calculations. It has been pointed out that the van der Waals interaction is important in this particular system.[31] Therefore, we calculated the detailed electronic structures by using DFT+D/PBE. The optimized structure of the G/Ru(0001) is shown in **Figure 1**(a) (top view) and (b) (side view). Each unit cell with 11×11 Ru(0001) and 12×12 graphene contains four different regions, fcc, hcp, atop, and bridge, in which the location of hexagonal holes of the graphene layer are on the fcc hollow, hcp hollow, top and bridge site of the Ru atoms in the first layer of the Ru(0001) substrate, respectively. Here, we focus on the electronic properties of different carbon atoms in these four regions. The projected density of states (PDOS) on p_z orbitals of different carbon atoms are shown in Figure 1(c), in which the C_a and C_b atoms (see the top-right inset in Figure 1(a)) denote the carbon atoms located on hollow and top sites of Ru(0001) in the fcc and hcp regions, respectively. We find that the intensity of the PDOS of C_a atoms at the Fermi level in fcc regions is much higher than that in other regions, implying a stronger sp^3 hybridization and a higher activity of the C_a atoms in fcc region, therefore, a stronger interaction with adsorbates.

The high activity of the C_a atoms in fcc region of G/Ru(0001) gives us an opportunity of growing dispersed nanoclusters on G/Ru(0001).[20–22] However, not all metals form dispersed nanoclusters on G/Ru(0001).[25,26] This suggests that the intrinsic electronic structure of the metals themselves also play a role in the growth mode. To determine the role of metal adsorbates we systematically investigated the configurations and corresponding electronic structures of several TM atoms on G/Ru(0001). In the following, we calculated the possible adsorption site for single metal atoms, Pt, Ru, Ir, Ti, Pd, Au, Ag, and Cu, on G/Ru(0001). As shown in the bottom-right inset in Figure 1(a), we define the possible adsorption sites for single atom adsorption on G/Ru(0001) using the graphene layer as a reference: B_1, B_2, T_1, T_2, and H sites, which denote the bridge of the nearest C_a and C_b atoms, the bridge of the two nearest C_a atoms, the top on a C_a or C_b atom and the hole of the benzene ring, respectively. To differentiate the adsorption sites at different regions of G/Ru(0001), for example, a H site in atop region, we denote it as H@atop.

The binding energies and adsorption sites of these single atoms on G/Ru(0001) are summarized in **Table 1**, where we find that all the metal atoms at fcc regions have larger binding energies. According to the magnitude of the binding energies, these transition metals can be divided into two groups: Pt, Ru, Ir, and Ti on G/Ru(0001) possess larger binding energies, while Pd, Au, Ag, and Cu have smaller ones. Because the four regions of G/Ru(0001) have different activities, these metals will prefer different adsorption sites in these four regions. For example, when one Pt atom absorbs on G/Ru(0001), the most stable adsorption site is B_2@fcc, while B_1@atop, B_1@bridge and B_2@hcp sites are less stable adsorption sites at atop, bridge, and hcp regions, respectively. For Ir, the less stable adsorption sites are T_2@fcc, T_2@hcp, H@bridge and H@atop. For Ti and Ru the H site is the most favorable one at all regions. For Au, Ag, and Cu in the second group with filled d orbitals, the most stable adsorption site is the T_1 site at all regions.

Considering the electronic structures of these atoms, the diversity of the adsorption sites can be attributed to the orbital occupation of TM atoms. For example, the metals in the first group have a partially filled d shell. Therefore, the frontier orbitals participating in the adsorption will be d orbitals. Considering the symmetry of d orbitals and the dangling bond of each C_a atom in the fcc region, the binding site will depend on the number and the symmetry of the unoccupied d orbitals. For example, the valence shell configuration of Ir is d^7s^2 with three unoccupied d orbitals, therefore the most stable configuration is that Ir atom bonds to three C_a atoms and is located on the T_2 site (Figure S1(a)). For Ru and Ti, the number of their unoccupied orbitals is larger than three (d^7s^1 for Ru,

Table 1. Binding energies and preferable adsorption sites (*Site*) for a group of transition metal atoms on G/Ru(0001) and on the freestanding graphene, where E_b is the binding energy, fcc, hcp, atop, bridge and graphene represent that the single atom is on fcc, hcp, atop, bridge region of G/Ru(0001) and freestanding graphene, respectively, E_{co} is the cohesive energy of the experiments.[32]

	Pt	Ru	Ir	Ti	Pd	Au	Ag	Cu
E_b (graphene)	2.85	4.37	3.42	3.96	1.89	0.94	0.52	1.06
E_b (atop)	2.92	4.52	3.71	4.15	1.95	1.04	0.55	1.13
E_b (hcp)	3.33	4.61	4.63	4.54	2.02	1.91	0.94	1.67
E_b (fcc)	3.54	5.04	5.01	5.01	2.07	1.96	1.11	1.69
E_b (bridge)	3.25	4.62	4.37	4.46	1.97	1.70	0.82	1.41
E_{co}	5.84	6.74	6.94	4.85	3.89	3.81	2.95	3.49
Site	B_1/B_2	H	T_2/H	H	B_1/B_2	T_1	T_1	T_1

d^2s^2 for Ti), thus the H site is their most stable adsorption site (Figure S1(b)). Because of the similar properties of electronic orbital occupation, Pd ($d^{10}s^0$) has the same adsorption site and smaller binding energy as Pt. This implies a difference in the actual adsorption process.[24] The frontier orbitals of Au, Ag, and Cu are $d^{10}s^1$ with a fully occupied *d* orbital and a half-occupied *s* orbital. It suggests that the electrons near the Fermi level, which will participate in the bonding with graphene, are *s* electrons. Considering the symmetry of the *s* orbital, Au, Ag and Cu will bind to a T_1 site (Figure S1(c)).

By comparing the frontier orbitals of these metal atoms, we find that the *d* orbitals for metals in the first group are not fully occupied, while the ones in the second group have a closed *d* shell. This implies that the unoccupied *d* orbitals play a significant role in the bonding of TM atoms on G/Ru(0001). Therefore, these metal atoms tend to adsorb on the site with high chemical activity, i.e., the fcc region of G/Ru(0001) in our case. It fits into this scheme that the binding energy of Pt in the fcc region is the largest one, which implies that Pt atoms will selectively adsorb at fcc regions of G/Ru(0001) at low coverage. The binding energies for metals with d^{10} configuration are much smaller because of the fully occupied *d* orbital. From experiments we know that Pt and Ru selectively adsorb on fcc region of G/Ru(0001) and form dispersed nanoclusters,[20–22] while Au tend to form a 2D layer. Work referenced in[25,26] is in good agreement with this rationalization.

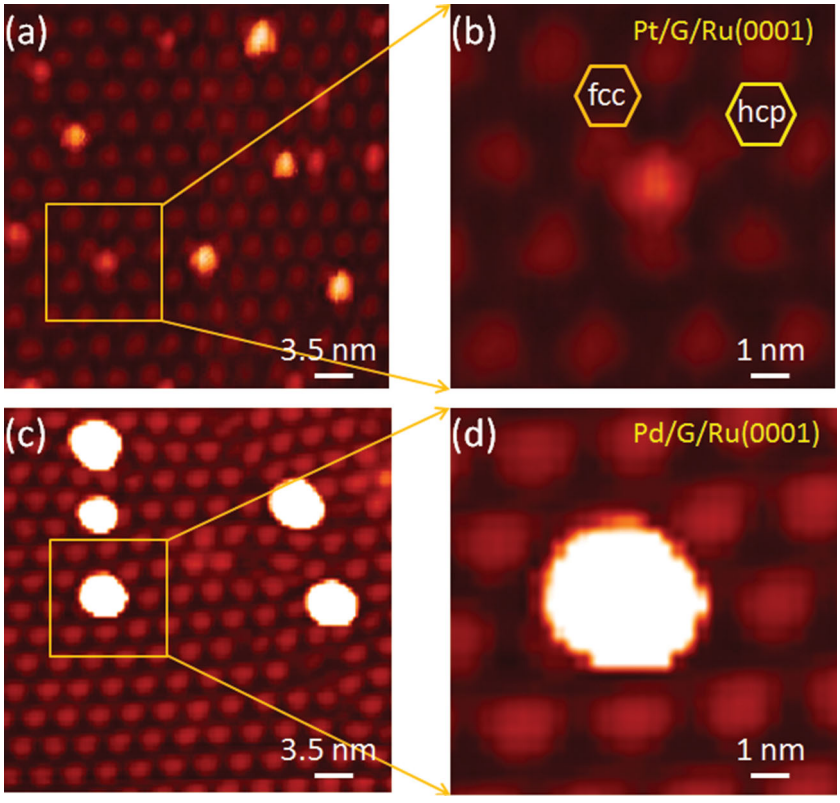

Figure 2. STM topographic image of (a) Pt nanoclusters (35 nm × 35 nm, $V_s = -1.2$ V, $I_s = -0.7$ nA) and (c) Pd clusters (35 nm × 35 nm, $V_s = -1.2$ V, $I_s = -0.09$ nA) on G/Ru(0001), (b) and (d) are the zoom-in view.

Experimental evidences of different growth pattern for Pt and Pd nanoclusters on G/Ru(0001) template are shown in **Figure 2**. We can clearly see that Pt forms nanoclusters at the fcc region, while Pd forms larger clusters and cross different regions. For Pt, it can be concluded that it follows the selection mechanism. But for Pd clusters on G/Ru(0001) in Figure 2(c) and (d), we find that Pd clusters cover different regions as a big island, no dispersed selective adsorption is observed. However, some groups reported that Pd could form dispersed nanoclusters at fcc region of G/Ru(0001) at very low temperature (150 K),[25] or at appropriate deposition rate.[23] According to our calculations, the binding energy of Pd at the fcc region of G/Ru(0001) is at the border of the first and second groups. For Au in the second group, it can only form layers on G/Ru(0001) at room temperature.[25,26] For Pt, and Ru in the first group, they all form the dispersed nanoclusters on G/Ru(0001) at room temperature.[20–22] Therefore, Pd could form either the dispersed clusters or metal layers at different experimental conditions (for example, different temperatures). It appears, then, that the binding energy of Pd at the fcc region of G/Ru(0001) can be considered as the critical energy. When the binding energy of the

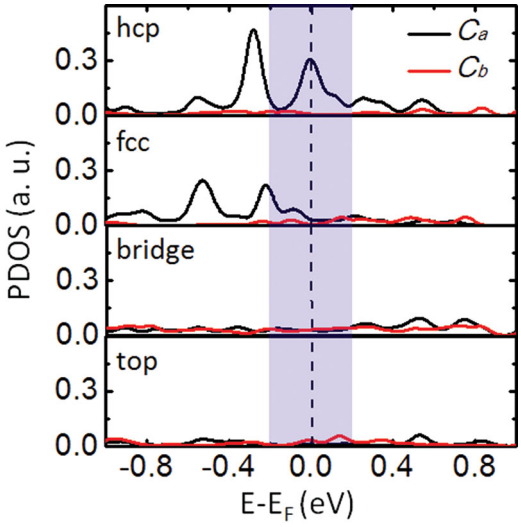

Figure 3. The projected density of states on p_z orbital (considering the vdW interaction) of C_a and C_b in the four regions of G/Rh(111).

single atom on G/Ru(0001) is larger or smaller than that of Pd, it can form the dispersed nanoclusters or atomic layers at the fcc region under the certain experimental conditions.

In **Figure 3**, we provide the DOS projected on a p_z orbital of graphene. It is clearly seen that there is strong local sp^3 hybridization at the hcp region, and the experimental results also show that the mono-dispersed metal clusters selectively cover the hcp regions.[24] We also find that its local sp^3 hybridization is weaker than that of at fcc region of G/Ru(0001). This means that the interaction between metal and G/Rh(111) is weaker than that between metal and G/Ru(0001). For example, according to our calculation, the binding energies of Pt atom at the fcc and hcp regions of G/Rh(111) are 2.79 eV and 2.97 eV, respectively (calculated by using DFT+D/PBE), which are smaller than the binding energies of Pt atom at fcc and hcp regions of G/Ru(0001) (Table S1).

To investigate the possible growth mode of the mono-dispersed nanoclusters for the metals in the first group, we use Pt on G/Ru(0001) as an example. The average binding energy (E_{ab}) is used to evaluate the growth mode of the Pt clusters. E_{ab} is defined as

$$E_{ab} = -(E_{tot} - E_{sub} - E_{metal} * n)/n, \quad (1)$$

where E_{tot} is the total energy of the Pt/G/Ru(0001) system, E_{sub} is the total energy of the G/Ru(0001) substrate, E_{metal} is the energy of the single Pt atom, and n is the number of the Pt atoms. The E_{ab} of Pt dimers and trimers are 4.25 eV and 4.51 eV, respectively. It implies that Pt atoms like to bond to each other at fcc region on G/Ru(0001). The fourth Pt atom aggregates with the remaining three in the same layer (binding energy 4.85 eV) rather than forming a pyramid on top of the three atoms in the first layer (binding energy 4.84 eV). This result illustrate that, at the fcc region, the Pt-C_a bond is stronger than the Pt-Pt bond and the Pt atoms initially tend to cover the fcc region, indicating the selective adsorption at the initial growth stage. **Figure 4**(i) shows the relationship between E_{ab} and the number of Pt atoms. In this figure, the black and red circles indicate the E_{ab} for the Pt atoms located in the first and the second layer. We find that E_{ab} increases with an increasing number of Pt atoms. After the Pt atoms have covered the whole fcc region, subsequent atoms will grow in the second layer because of larger E_{ab} (e.g., the E_{ab} of the configuration with 16 Pt atoms cover the whole fcc region and some of the bridge region in one layer state (Figure 4(g)) is 5.65 eV, which is about 40 meV smaller than that of the configuration with some atoms located at the second layer (Figure 4(h))). This layer by layer growth mode agrees well with the experimental observation.[20]

3. Conclusion

In general, the growth mechanism of transition metal atoms on a G/metal template can be summarized as follows: both the local sp^3 hybridization of the substrate and the occupation of the outermost orbital (for example, d orbital for transition metals) of the adsorbates determine the interaction between the adsorbates and the G/metal, and thus determine the morphology of the adsorbates. If the adsorbate has a partially occupied outermost orbital and the corresponding G/metal has strong sp^3 hybridization at specific regions (for example, fcc region of G/Ru(0001)), it will form dispersed nanoclusters. Otherwise, it will form large islands across different regions or metal layers. Meanwhile, it is found that the binding energy of Pd on the fcc region of G/Ru(0001) (≈2 eV) could be the critical limit between growing dispersed metal nanoclusters or islands on G/Ru(0001). By using Pt as an example, we investigated the growth mode of the Pt nanoclusters on G/Ru(0001). Here, the proposed growth mechanism agrees well with our experimental observations. Our work provides a predictive method to select suitable metal atoms and G/metal templates for the growth of dispersed metal nanoclusters, aimed at applications in catalysis.

4. Theoretical and Experimental Section

Theoretical Methods: All density functional theory calculations were carried on by using Vienna ab initio simulation package (VASP).[33,34]

For G/Ru(0001) and G/Rh(111), we use the DFT+D/PBE[36] (in which the Grimme's empirical dispersion correction scheme was taken into account) to do the structural relaxations and electronic structure calculations. The standard values of the GGA calculation parameters are used in these DFT+D/PBE calculations.[37,38] The periodic slab models include three layers of metal, one layer of graphene, and a vacuum layer of 15 Å. All the atoms except the bottom two layers of Ru(0001) were fully relaxed until the net force on each relaxed atom was less than 0.01 eV/Å. A Γ point k-sampling was employed for Brillouin zone matrix integrations due to the numerical limitations. The DFT+D/PBE calculation results agree with those by GGA method qualitatively,[29,30] and lead to much more accurate PDOS due to the appropriate distance between graphene and Ru(0001) substrate.[31]

For metal/G/Ru(0001), we only performed LDA calculations, as this level of theory provides appropriate description of binding energies and growth modes, when investigating Ir

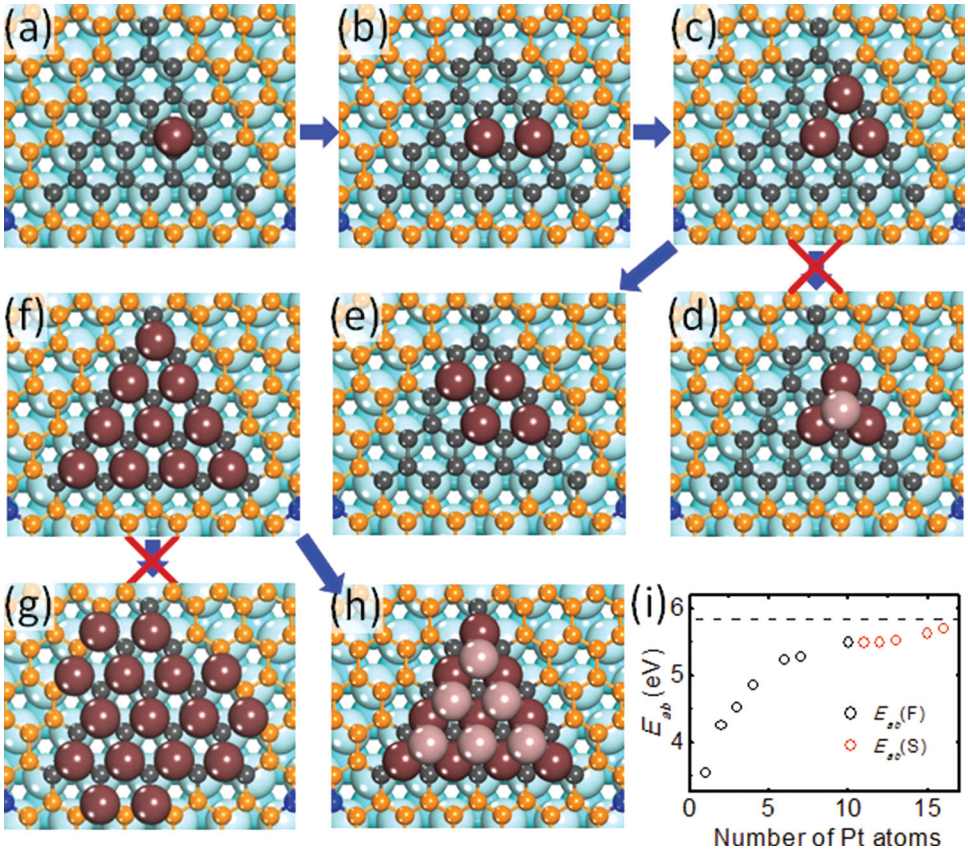

Figure 4. Schematics of the layer by layer growth path of Pt nanoclusters on the fcc region of the G/Ru(0001) from one Pt atom (a) to sixteen Pt atoms (g) and (d) shows the metastable configurations for four and sixteen Pt atoms on G/Ru(0001). (h) The stable configuration of sixteen Pt atoms on G/Ru(0001). (i) Average binding energy (E_{ab}) vs the number of the Pt atoms, the black and red squares show the E_{ab} of Pt atoms located at the first and second layer, respectively, where the dashed line at 5.84 eV shows the cohesive energy of Pt. [32]

nanoclusters on G/Ir(111).[27,28] We also calculated the Pt/G/Ru(0001) systems by using DFT+D/PBE, and find the same adsorption sites and similar trend of binding energies as by using LDA,[35] that is, the Pt atom at fcc region has the largest binding energy (Table S1). LDA calculations use fewer layers of substrate leading to the similar geometric structures and electronic structures (Figure S2 and Figure S3) to DFT+D/PBE calculations (Figure 1) for the G/Ru(0001) system. Hence we used LDA to calculate the metal/G/Ru(0001) systems.[35] The energy cutoff of the plane-wave basis sets was 400 eV. The periodic slab model contains two layers of 11×11 Ru(0001), one layer of 12×12 graphene, and a vacuum layer of 15 Å. All the atoms except the bottom layer of Ru(0001) were fully relaxed until the net force on each relaxed atom was less than 0.01 eV/Å. A Γ point k-sampling was employed for Brillouin zone matrix integrations due to the numerical limitations.

It's well known that the strain effect will induce mono-dispersed metal island growth on other substrates.[39] In this work, the influence of strain effect coming from lattice mismatch between Pt and G/Ru(0001) substrate on the electronic structures is also considered in our DFT calculations.

Experimental Methods: Experiments were carried out in a standard ultrahigh vacuum (UHV) system with base pressure lower than 1×10^{-10} mbar. The single graphene layer was grown on Ru(0001) surface by carbon segregation, which was presented in detail elsewhere.[10] Pt/Pd was deposited onto the template from a Pt/Pd rod (purity of 99.99%) mounted on the evaporator, with a constant deposition rate 0.01 ML/min (1 ML = 1.6×10^{15} atoms/cm^2) by monitoring the ion current flux of the Pt/Pd vapor beam. Then the sample was studied with room temperature scanning tunneling microscope (STM) at constant current mode.

Supporting Information

Configurations for Au, Ir and Ti on G/Ru(0001) (Figure S1), configurations (Figure S2) and PDOS (Figure S3) for G/Ru(0001), calculated by using LDA, and binding energies and adsorption sites for Pt atom on G/Ru(0001), calculated by using DFT+D/PBE (Table S1). This material is available from the Wiley Online Library or from the author.

Acknowledgements

This work was partially supported by the Natural Science Foundation of China (NSFC), the MOST 973 projects of China, the Chinese Academy of Sciences (CAS), Shanghai Supercomputer Center.

Received: November 6, 2013
Revised: January 26, 2014
Published online: February 20, 2014

[1] W. A. de Heer, *Rev. Mod. Phys.* **1993**, *65*, 611.
[2] H.-G. Boyen, G. Kästle, F. Weigl, B. Koslowski, C. Dietrich, P. Ziemann, J. P. Spatz, S. Riethmüller, C. Hartmann, M. Möller, G. Schmid, M. G. Garnier, P. Oelhafen, *Science* **2002**, *297*, 1533.
[3] L. Lee, F. Delbecq, R. Morales, M. A. Albiter, F. Zaera, *Nat. Mater.* **2009**, *8*, 132.
[4] B. C. Gates, *Chem. Rev.* **1995**, *95*, 511.
[5] N. Nilius, E. D. L. Rienks, H.-P. Rust, H.-J. Freund, *Phys. Rev. Lett.* **2005**, *95*, 066101.
[6] A. T. N'Diaye, S. Bleikamp, P. J. Feibelman, T. Michely, *Phys. Rev. Lett.* **2006**, *97*, 215501.
[7] D. Franz, S. Runte, C. Busse, S. Schumacher, T. Gerber, T. Michely, M. Mantilla, V. Kilic, J. Zegenhagen, A. Stierle, *Phys. Rev. Lett.* **2013**, *110*, 065503.
[8] Y. Pan, D. X. Shi, H.-J. Gao, *Chinese Physics* **2007**, *16*, 3151.
[9] P. W. Sutter, J. Flege, E. A. Sutter, *Nat. Mater.* **2008**, *7*, 406.
[10] Y. Pan, H. G. Zhang, D. X. Shi, J. T. Sun, S. X. Du, F. Liu, H.-J. Gao, *Adv. Mater.* **2009**, *21*, 2777.
[11] B. Wang, M. Caffio, C. Bromley, H. Früchtl, R. Schaub, *ACS Nano* **2010**, *4*, 5773.
[12] M. Gao, Y. Pan, L. Huang, H. Hu, L. Z. Zhang, H. M. Guo, S. X. Du, H.-J. Gao, *Appl. Phys. Lett.* **2011**, *98*, 033101.
[13] D. Martoccia, P. R. Willmott, T. Brugger, M. Björck, S. Günther, C. M. Schlepütz, A. Cervellino, S. A. Pauli, B. D. Patterson, S. Marchini, J. Wintterlin, W. Moritz, T. Greber, *Phys. Rev. Lett.* **2008**, *101*, 126102.
[14] B. Wang, S. Günther, J. Wintterlin, M.-L. Bocquet, *New J. Phys.* **2010**, *12*, 043041.
[15] H. G. Zhang, J. T. Sun, T. Low, L. Z. Zhang, Y. Pan, Q. Liu, J. H. Mao, H. T. Zhou, H. M. Guo, S. X. Du, F. Guinea, H.-J. Gao, *Phys. Rev. B* **2011**, *84*, 245436.
[16] J. H. Mao, H. G. Zhang, Y. H. Jiang, Y. Pan, M. Gao, W. D. Xiao, H.-J. Gao, *J. Am. Chem. Soc.* **2009**, *131*, 14136.
[17] A. J. Pollard, E. W. Perkins, N. A. Smith, A. Saywell, G. Goretzki, A. G. Phillips, S. P. Argent, H. Sachdev, F. Müller, S. Hüfner, S. Gsell, M. Fischer, M. Schreck, J. Osterwalder, T. Greber, S. Berner, N. R. Champness, P. H. Beton, *Angew. Chem. Int. Ed.* **2010**, *49*, 1794.
[18] A. T. N'Diaye1, T. Gerber, C. Busse, J. Mysliveček, J. Coraux, T. Michely, *New J. Phys.* **2009**, *11*, 103045.
[19] A. Cavallin, M. Pozzo, C. Africh, A. Baraldi, E. Vesselli, C. Dri, G. Comelli, R. Larciprete, P. Lacovig, S. Lizzit, D. Alfè, *ACS Nano* **2012**, *6*, 3034.
[20] Y. Pan, M. Gao, L. Huang, F. Liu, H.-J. Gao, *Appl. Phys. Lett.* **2009**, *95*, 093106.
[21] K. Donner, P. Jakob, *J. Chem. Phys.* **2009**, *131*, 164701.
[22] E. Sutter, P. Albrecht, B. Wang, M.-L. Bocquet, L. Wu, Y. Zhu, P. Sutter, *Surf. Sci.* **2011**, *605*, 1676.
[23] B. Wang, B. Yoon, M. König, Y. Fukamori, F. Esch, U. Heiz, *Nano Lett.* **2012**, *12*, 5907.
[24] M. Sicot, S. Bouvron, O. Zander, U. Rüdiger, Yu. S. Dedkov, M Fonin, *Appl. Phys. Lett.* **2010**, *99*, 093115.
[25] Z. Zhou, F. Gao, D. W. Goodman, *Surf. Sci.* **2010**, *604*, L31.
[26] L. Liu, Z. H. Zhou, Q. L. Guo, Z. Yan, Y. X. Yao, D. W. Goodman, *Surf. Sci.* **2011**, *605*, L47.
[27] P. J. Feibelman, *Phys. Rev. B* **2008**, *77*, 165419.
[28] P. J. Feibelman, *Phys. Rev. B* **2009**, *80*, 085412.
[29] B. Wang, M.-L Bocquet, *J. Phys. Chem. Lett.* **2011**, *2*, 2341.
[30] B. Wang, M.-L. Bocquet, S. Marchini, S. Günther, J. Wintterlin, *Phys. Chem. Chem. Phys.* **2008**, *10*, 3530.
[31] D. Stradi, S. Barja, C. Díaz, M. Garnica, B. Borca, J. J. Hinarejos, D. Sánchez-Portal, M. Alcamí, A. Arnau, A. L. Vázquez de Parga, R. Miranda, F. Martín, *Phys. Rev. Lett.* **2011**, *106*, 186102.
[32] C. Kittel, *Introduction to Solid State Physics*, 8th ed. Wiley, New York **2005**.
[33] J. P. Perdew, A. Zunger, *Phys. Rev. B* **1981**, *23*, 5048.
[34] G. Kresse, J. Furthmuller, *Phys. Rev. B* **1996**, *54*, 11169.
[35] D. M. Ceperley, B. J. Alder, *Phys. Rev. Lett.* **1980**, *45*, 566.
[36] S. Grimme, *J. Comput. Chem.* **2006**, *27*, 1787.
[37] J. P. Perdew, K. Burke, M. Ernzerhof, *Phys. Rev. Lett.* **1996**, *77*, 3865.
[38] T. Bučko, J. Hafner, S. Lebègue, J. G. Ángyán, *J. Phys. Chem. A* **2010**, *114*, 11814.
[39] F. Liu, *Phys. Rev. Lett.* **2002**, *89*, 246105.